5th SASTech
Iran | Mashhad
May 12 - 17 | 2011
5th Symposium on Advances in Science & Technology

Distance preserving dimensionality reduction methods and their applications in geometric inspection of nonrigid parts

Hassan RADVAR-ESFAHLAN[1,a] ; Souheil-Antoine TAHAN[1,b]
[1] École de Technologie Supérieure, Montréal, Canada
[a] hassan.radvar-esfahlan.1@ens.etsmtl.ca
[b] antoine.tahan@etsmtl.ca

Abstract

Freeform surfaces in automotive and aerospace industries are now widely used in all engineering design disciplines from consumer goods products to ships. The parts with a very thin wall in proportion to their size are referred to as nonrigid (or flexible) parts. Generally, for the dimensional and geometric inspection of such parts, *special inspection fixtures*, in combination with tridimensional measuring systems (CMM, laser, etc.), are used because these parts may have different shapes in a *free state* from the design model (CAD) due to inherent variations of manufacturing process, gravity loads and residual strains. The aim of this study is to develop new methodology to eliminate the use of inspection fixtures. This study elaborates on the theory and general methods for the metrology of nonrigid parts. We will merge existing technologies in metric and computational geometry, nonlinear dimensionality reduction, and finite element method to develop a general approach to the geometrical inspection of nonrigid parts.

Key words: Geometric inspection, Compliant part, Nonlinear dimensionality reduction.

1. Introduction

The traditional method in automotive and aircraft industries for inspection of flexible parts is to inspect precision components involving freeform surfaces by combining the inspection fixture and coordinate measuring machine (CMM). Non-contact 3D digitizing systems exposed a new horizon in industrial inspection of both rigid and nonrigid parts. Three-dimensional optical digitizing systems are suitable for the measurement of large-sized flexible parts for they allow non-contact measurement and are able to deliver, in a relatively short time, large clouds of points that are representative of object surfaces. The part is setup on a portable 3D optical digitizing system which is installed in a production line regardless of datum shown in the engineering drawings. Due to weight, and of course supports, part deformations occur. An identification method must be defined in order to extract geometrical profile deviations due to manufacturing defects while simulating the *use state* to compensate for a spring-back effect and gravity. The remainder of this paper presents the theory and methods for geometric inspection in nonrigid parts.

2. Background

2.1 Geometric inspection of nonrigid parts

A state of the art review of the most important measuring techniques is presented in Savio *et al.* [1] along with their capacity for freeform measuring tasks. Weckenmann and Gabbia [2] proposed a measuring method using virtual distortion compensation. They used the measurement results to extract object features like holes or edges. Some of these were relevant to the assembly process; others were subject to further inspection. From the information about the transformation of assembly features from their actual to their nominal position, virtual distortion compensation was used to calculate feature parameters of the distortion compensated shape. Their method was not completely automated because the suggested method needed some human challenges to identify the correlation between some special points like holes and assembly joint positions. These led the controller to find the boundary conditions of the FEM problematic. Besides, transforming the point cloud to a computer-aided analyzable model is a very time consuming process. The concept of the *Small Displacement Torsor* (SDT) was developed by Bourdet and Clément [3] to solve the general problem of a geometrical surface model fit to a set of points using rigid body movements. Lartigue *et al.* [4] took advantage of the possibilities offered by voxel representation and SDT method for the dimensional metrology of flexible parts. This time, they considered the effect of gravity and the spatial location of a scanned part. This method is fundamentally based on finding the correspondence between the cloud of all measured points and CAD meshed data. In fact, the SDT is more suitable for small deformations.

2.2 Rigid and nonrigid surface registration

Besl and Mckay [5] developed an iterative method for the rigid registration of 3D shapes. The ICP algorithm is one of the common techniques for the refinement of partial 3D surfaces (or models) and many variant techniques have been investigated [6, 7]. Shi *et al.* [8] pointed out that ICP-based algorithms may not fit inspection applications because the transformation matrix for registration is estimated in a way that total shape error is minimized. This cannot be applied to industrial quality control. The *Fast Marching Method* was introduced by Sethian [9-11] as a computationally efficient solution to *Eikonal equations* on flat domains. The fast marching method was extended to triangulated surfaces by Kimmel and Sethian [12]. The extended method solved the Eikonal equation on flat rectangular, or curved triangulated, domains. Elad and Kimmel [13] presented the concept of *Invariant Signature* for surfaces. Their method used fast marching on triangulated domains followed by *Multidimensional Scaling* (MDS) technique. They practically transformed the problem of isometric-nonrigid surface matching into a matching of rigid surfaces problem. Using MDS, they embedded surfaces *X* and *Y* into some common embedding space *Z* called *Canonical form* and then measured their similarity using the *Hausdorff distance*. Their method is strongly based on the Kimmel and Sethian [12] method in computing the geodesic distance on triangular meshes. In fact, Euclidean embedding is rarely without distortion. Cox and Cox [14] showed how points of a configuration from non-metric MDS can be forced to lie on the surface of a sphere.

2.3 Nonlinear dimensionality reduction

Any manifold can be fully described by pairwise distances. This is the motivation behind the distance preserving nonlinear dimensionality reduction. Sammon [15] proposed a *nonlinear mapping algorithm* (NLM), a useful tool in pattern recognition, as a projection

method for analyzing multivariate data. The method attempts to find a low-dimensional representation of a set of points distributed in a high dimensional pattern space, such that the Euclidean distance between points in the map are as similar as possible to the Euclidean distance between the corresponding points in the high-dimensional pattern space. Actually, NLM is closely related to metric MDS. A disadvantage of original NLM is that it, unlike for example Principal Component Analysis (PCA), does not yield a mathematical or algorithmic mapping procedure for previously unseen data points. That is, when a new point has to be mapped, the whole mapping procedure has to be repeated [16]. The *Sammon artificial neural network* (SAMANN) [17] optimizes the same error (stress) function achieves it in a completely different way. Instead of minimizing the stress function as such with a steepest descent method, which leads to a discrete mapping of the data set, this method propose establishing an implicit mapping between the initial space and the final space. The (Kohonen's) *Self-Organizing Map* (SOM) [18] combines a competitive learning principle with a topological structuring of nodes such that adjacent nodes tend to have similar weight vectors. Competitive learning requires inhibitory connections among all nodes; topological structuring implies that each node also has excitatory connections to a small number of nodes in the network. The topology is specified in terms of a neighborhood relation among nodes. The SOM converts complex, nonlinear relationships in the high-dimensional space into simpler geometric relationships such that the important topological and metric relationships are conveyed. The data are organized on the grid in such a way that observations that are close together in the high-dimensional space are also closer to each other on the grid. Thus, this is very similar to the ideas of MDS, except that the positions in the low-dimensional space are restricted to the grid. The improvement to NLM was brought by Demartines and Hérault [19] in order to underline the nonlinear capabilities of their method, they call it *Curvilinear Component Analysis* (CCA), by opposition with PCA. CCA is more powerful and faster than Sammon's mapping. Curvilinear component analysis is a self-organized neural network that encompasses two main steps. First, there is a vector quantization step [20] where input vectors become prototypes of the distribution. The next step is to find a nonlinear projection of the quantizing (or codebook) vectors by minimizing a cost function based on interpoint distances in the input and output spaces. In fact, CCA combines aspects of MDS and SOM to unfold the data and reveal interesting structure.

3. Theoretical foundation

3.1 Metric spaces

Let X and Y be metric spaces and $f: X \rightarrow Y$ an arbitrary map. The *distortion* of f is defined by:

$$\text{dis } f = \sup_{a.b \in X} \left| d_Y(f(a), f(b)) - d_X(a,b) \right| \tag{1}$$

The distance $d_X(a,b)$ between a pair of points in X is mapped to the distance $d_Y(f(a), f(b))$ between the images of a and b under f. For a complete *Riemannian manifold*, the metric $d(a,b)$ is defined as the length of the shortest curve (*geodesic*) between a and b.We denote X and Y as subsets of a metric space (Z,d_Z). The *Hausdorff distance* between X and Y, $d_H(X, Y)$, is defined by:

$$d_H(X,Y) = \max\left(\sup_{x \in X} \inf_{y \in Y} d_Z(x,y), \sup_{y \in Y} \inf_{x \in X} d_Z(x,y) \right) \tag{2}$$

and *Gromov-Hausdorff* distance between two metric spaces (X, dx) & (Y, dy) is defined as:

$$d_{GH}(X,Y) = \inf_{Z,f,g}\left(d_H^Z(f(X),g(Y))\right) \tag{3}$$

where f: $X \rightarrow Z$ and g: $Y \rightarrow Z$ are isometric embeddings (distance preserving) into the metric space (Z,d). The d_{GH} satisfies the triangle inequality, i.e. ,

$$d_{GH}(X_1,X_3) \le d_{GH}(X_1,X_2) + d_{GH}(X_2,X_3) \tag{4}$$

for any metric spaces X_1 , X_2 , X_3. Moreover d_{GH} $(X, Y) = 0$ if, and only if, X and Y are isometric.

3.2 Isometric embedding

In order to compare the nonrigid shapes we should look at their intrinsic geometries because they rest unchanged during isometric deformations. Consider X and Y as two metric shapes (Fig. 1).

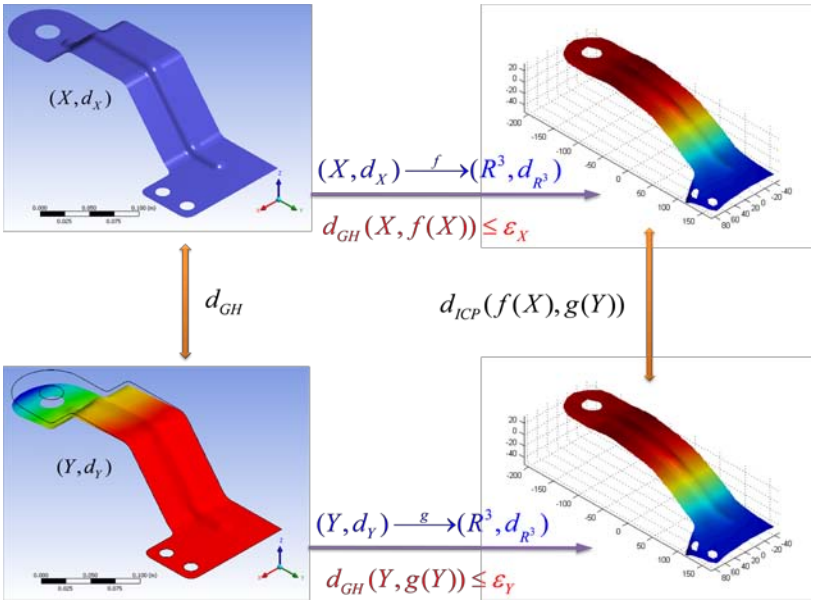

Figure 1: Canonical form distance.

Let us compute the *Canonical Form* (CF) as:

$$\begin{aligned} f &= \arg\min_{f:X\to\square} dis\ f \quad \rightarrow \quad Z(X) = f(X) \\ g &= \arg\min_{g:Y\to\square} dis\ g \quad \rightarrow \quad Z(Y) = g(Y) \end{aligned} \tag{5}$$

and compare the extrinsic geometries of canonical forms,

$$d_{CF}(X,Y) = d_{ICP}(Z(X),Z(Y)) = \min_{\substack{f:X\to\square \\ g:Y\to\square}} d_H^{\square}(f(X),g(Y)) \tag{6}$$

The term canonical form, computed as Hausdorff distance between the minimum distortion embeddings of two shapes X and Y into some common metric space (Z,d_Z), is used as well. In fact, canonical form is the extrinsic representation of the interensic geometry of shape X, and using this, we can transform our nonrigid shape similarity into the rigid similarity problem. As a corollary of Gauss's *Theorema Egregium*, a piece of paper cannot be bent onto a sphere without crumpling. Conversely, the surface of a sphere cannot be unfolded onto a flat plane without distorting the distances. Although a truly isometric embedding of shape X is not always possible, we can try to construct an approximate representation of X by minimizing the *distortion* as we defined in equation

(1). In our point cloud setting, where the shape X is sampeled at N points $\{x_1,x_2,\ldots,x_N\}$, the distortion criteria will be:

$$\sigma = \max_{i,j=1,\ldots,N} \left| d_{\square^m}(f(x_i), f(x_j)) - d_X(x_i, x_j) \right| \tag{7}$$

The function σ which measures the distortion of distances is called *stress*. As a routine σ_2 is used as the distortion criterion. Considering $Z_i = f(x_i)$ an $N \times m$ matrix of canonical form coordinates and $d_{ij}(Z) = d_{\square^m}(z_i, z_j)$, then:

$$\sigma_2(Z; D_X) = \sum_{i>j} \left| d_{ij}(Z) - d_X(x_i, x_j) \right|^2 \tag{8}$$

Where $D_X = d_X(x_i, x_j)$ is a $N \times N$ matrix of geodesic distances and $d_{ij}(Z)$ is the Euclidean distance between the points on the canonical form. Using this formulation, the coordinates of discrete canonical forms are the solution to the nonlinear least-squares problem:

$$Z^* = \arg\min_{Z \in \square^{N \times m}} \sigma_2(Z) \tag{9}$$

The SMACOF algorithm [14] (Scaling by MAjorizing a Complicated Function) can be used to minimize the (Kruskal) stress function.

3.3 Curvilinear component analysis

The CCA stress function is closely resembles Sammon's stress function:

$$E_{CCA} = \frac{1}{2} \sum_{\substack{i=1 \\ j=1}}^{N} (d(x_i, x_j) - d(y_i, y_j))^2 F(d(y_i, y_j), \lambda_y) \tag{10}$$

While we would like to have $d(x_i, x_j) = d(y_i, y_j)$, this is not always possible at all scales, so a weighting function was introduced. Generally, $F(d(y_i, y_j), \lambda_y)$ is chosen as a bounded and monotonically decreasing function in order to preserve the local topology in the new space. Demartines and Hérault [19] used the following in the simulation:

$$F\left(d(y_i, y_j), \lambda_y\right) = \begin{cases} 1 & if\ d(y_i, y_j) \le \lambda_y \\ 0 & if\ d(y_i, y_j) > \lambda_y \end{cases} \tag{11}$$

Decreasing exponential and sigmoid function also can be used. The hyperparameter λ_y is similar to the neighborhood radius in SOM, and it changes as the minimization of equation (11) proceeds. This is typically driven by an automatic schedule, but the original paper describes how it can be chosen in interactive manner. The minimization of stress function was achieved by novel variant of gradient descent methods. They used vector quantization where the original data are represented by a smaller set of prototype vectors. By this means they reduced the computation time. Other advantage of their optimization method is that the stress function can temporarily increase, which allows the algorithm to escape from a local minima.

4. Nonrigid geometric inspection

4.1 Assumptions

In this paper we assume the following.

1. The surface that is sampled is a valide surface.
2. There is a finite set of points that sample the surface.

3. The input sampled point set, reflects only the positions of the points on the surface and there is no duplication of sample points.
4. We assume that any small perturbation of the point locations does not change the connectivity in the reconstructed surface. This point will be discussed later.
5. The diverse methods for meshing will not be discussed and we assume that such (triangualr) meshing exists for range data and CAD surface.
6. We assume that profile defect is not situated at the boundary of part.
7. We assume that there is a bijective mapping between range data and CAD-model.

4.2 Inspection algorithm

Assuming the availability of scanned point clouds, the goal is to register two clouds of points, the first belongs to a CAD model and the second belongs to range data obtained in free-state. For flexible parts and before scanning, one should take into consideration the effect of spatial positioning (part set-up) in the final geometrical form of scanned data. Without knowing the important fact of gravity direction, serious errors in results can be predicted. Thus, before scanning, the part is setup onto reference support points in which their position is clearly defined within the part frame. Note that the set-up must not be over-constrained, unless otherwise specified according to designer request (ISO 10579). In this case, the same constraints must be taken into consideration during finite element analysis. Let X and Y be metric spaces with metrics dx and dy; the first correspond to the CAD model and the second to scanned range data. Due to the fact that x_i and y_i belong to two different metric spaces; similarity measure cannot be computed using Hausdorff distance. In order to compare these two spaces we mapped them into common metric space Z. Instead of Euclidean pairwise distance for the input of least square MDS algorithm, we used the geodesic distances between all pairs of points on surface. To this end, we used the fast marching method on triangulated domains. We used the SMACOF algorithm for minimizing the stress. Next step is mapping the output of least square MDS into plane using CCA strategy. At this stage we used the pairwise geodesic distance between all points in meshed surfaces as an input for CCA. At the end we used the Procrustes analysis as similarity measure, which has been used for statistical shape analysis and image registration of 2D/3D data, removes the translational, rotational and scaling components from one set so that the optimal alignment between the two sets can be achieved. Finally, we suppose that there is no a priori information for the assembly process. So, the contour can be used for mapping the preprocessed CAD-model into the range data. Defects due to geometric deviation can be found after finite element nonrigid registration, eliminating the spring-back effect. Proposed algorithm is illustrated in Fig. 2.

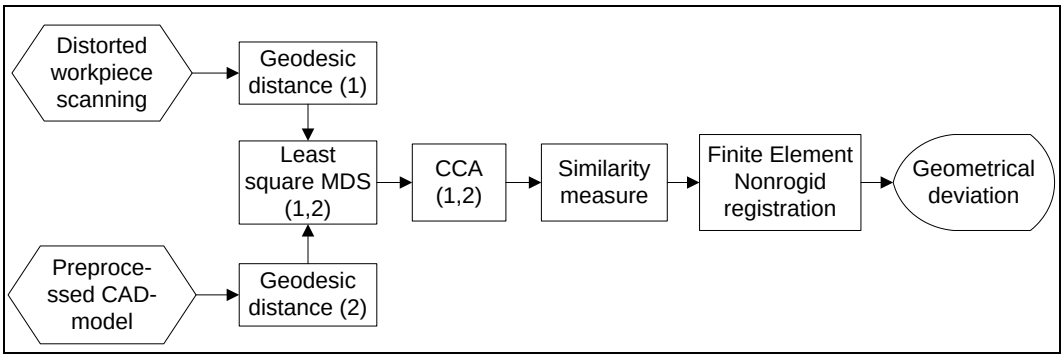

Figure 2: Numerical inspection algorithm.

5. Results

We have tested presented methodology in a series of typical mechanical parts. This section presents only one case study (at two stages) as a sample that evaluates performance and validates the method developed in previous section. To this end, a free-form model is simulated by CATIA® and ANSYS® then a finite element analysis of the model is done simulating the free-state range data. At this step, an external force is applied to the model to simulate unknown spring back deformation. Due to the fact that we have used predefined deformation in range data generation steps (spring back and profile defect), qualitative performance evaluation is effectively traceable. At first, deformed -but defectless- range data was evaluated. In fact every proposed algorithm should approve this defectless scanned part. In this case every calculated deviation shows the accuracy of method (Fig. 3d). To this end, we performed the proposed numerical inspection algorithm (Fig. 2), and the results are shown in Fig. 3. To evaluate the performance of proposed algorithm in finding the imposed local deviation, scanned part was contaminated by a local deviation of 8 mm. Then a topological Gaussian noise N(0,0.03 mm) was added on it. The algorithm was tested again and the maximum deviation of 7.78 was measured.

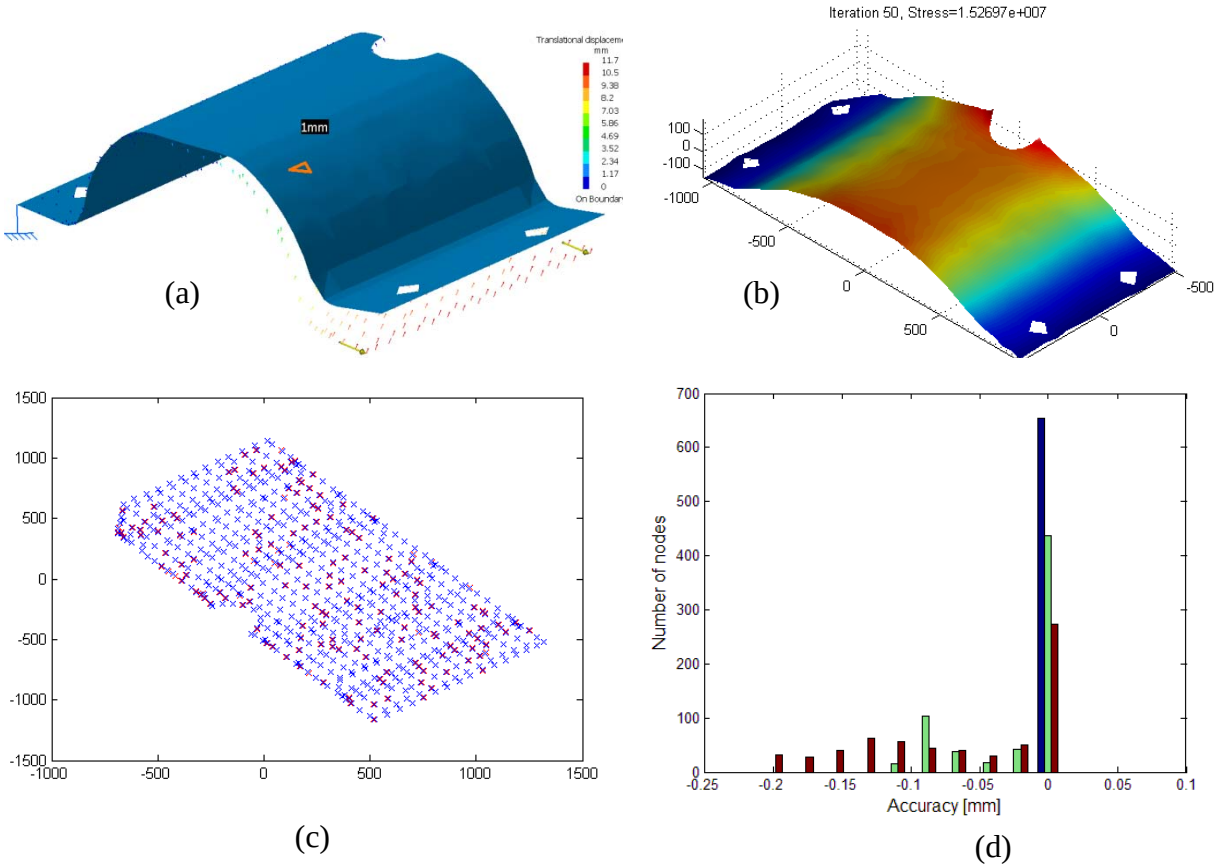

Figure 3: Similarity measure.
(a) Simulation of spring back effect (11.7 mm deformation). (b) Least square MDS. (c) CCA followed by Procrustes analysis. (d) Accuracy of method (obtained with defectless scanned part).

6. Conclusion

This paper presented a new strategy for the inspection of surface profiles of flexible parts without the use of specialized fixtures. We merged the technologies in metric and computational geometry along with nonlinear dimensionality reduction methods and finite element method to develop a general approach to the geometrical inspection of nonrigid parts. Despite the fact that the proposed method was quite efficient, there is plenty of work

to do for future computational speedup and accuracy. As a matter of fact, the proposed method is not a perfect and faultless substitution for inspection fixtures and CMM reports. Although we have tried to present convincing results, no method with such promise is likely to be widely accepted until more practical testing can be done. We assume that there is a bijective mapping between scanned point cloud and CAD-model. In fact this hypothesis is rarely exists in engineering applications. Future works should focus on this drawback. Although there were few researches in geometric inspection of nonrigid parts, general-purpose, fully automated and practical method does not yet exist. Specific long-term goals must be set forth and systematically accomplished.

Acknowledgement
The authors would like to thank the *National Sciences and Engineering research Council* (NSERC) for support and financial contribution.

References

[1] E. Savio, *et al.*, "Metrology of freeform shaped parts," *CIRP Annals-Manufacturing Technology,* vol. 56, pp. 810-835, 2007.

[2] A. Weckenmann and A. Gabbia, "Testing formed sheet metal part using fringe projection and evaluation by virtual distortion compensation," in *The 5th Inter Workshop on Automatic Processing of Fringe Patterns,* 2005.

[3] P. Bourdet and A. Clément, "Controlling a complex surface with a 3 axis measuring machine," *Annals of the CIRP,* vol. 25, pp. 359-361, 1976.

[4] C. Lartigue, *et al.*, "Dimensional metrology of flexible parts: Identification of geometrical deviations from optical measurements," in *Advanced mathematical & computational tools in metrology VII*, ed., p. 196, 2006.

[5] P. Besl and H. McKay, "A method for registration of 3-D shapes," *IEEE Trans on pattern analysis and machine intelligence,* vol. 14, pp. 239-256, 1992.

[6] J. Bentley, "Multidimensional binary search trees used for associative searching," *Communications of the ACM,* vol. 18, p. 517, 1975.

[7] S. Rusinkiewicz and M. Levoy, "Efficient variants of the ICP algorithm," *Int Conf on 3-D Digital Imaging and Modeling (3DIM '01)* pp. 145–152, 2001.

[8] Q. Shi, *et al.*, "Registration of Point Clouds for 3D Shape Inspection," *Intelligent robots and systems, 2006 IEEE/RSJ* pp. 235-240, 2006.

[9] J. Sethian, "A fast marching level set method for monotonically advancing fronts," *Procs of the National Academy of Sciences,* vol. 93, p. 1591, 1996.

[10] J. Sethian, *Level set methods and fast marching methods*: Cambridge university press Cambridge, 1999.

[11] J. Sethian, "Theory, algorithms, and applications of level set methods for propagating interfaces," *Acta numerica,* vol. 5, pp. 309-395, 2008.

[12] R. Kimmel and J. Sethian, "Computing geodesic paths on manifolds," *Proc. Natl. Acad. Sci. USA,* vol. 95, pp. 8431–8435, 1998.

[13] A. Elad and R. Kimmel, "On bending invariant signatures for surfaces," *IEEE Transactions on pattern analysis and machine intelligence,* vol. 25, pp. 1285-1295, 2003.

[14] M. Cox, *Multidimensional scaling*: CRC Press, 2000.

[15] J. W. Sammon Jr, "A nonlinear mapping for data structure analysis," *Computers, IEEE Trans,* vol. 100, pp. 401-409, 2006.

[16] D. De Ridder and R. P. W. Duin, "Sammon's mapping using neural networks: a comparison," *Pattern Recognition Letters,* vol. 18, pp. 1307-1316, 1997.

[17] J. Mao and A. K. Jain, "Artificial neural networks for feature extraction and multivariate data projection," *Neural Networks, IEEE Trans,* vol. 6, pp. 296-317, 2002.

[18] T. Kohonen, "Self-organized formation of topologically correct feature maps," *Biological cybernetics,* vol. 43, pp. 59-69, 1982.

[19] P. Demartines and J. Hérault, "Curvilinear component analysis: A self-organizing neural network for nonlinear mapping of data sets," *Neural Networks, IEEE Trans,* vol. 8, pp. 148-154, 2002.

[20] S. C. Ahalt, *et al.*, "Competitive learning algorithms for vector quantization" *Neural Networks,* vol. 3, pp. 277-290, 1990.